Special Aspects of Pharmacokinetics of Inhalation Anesthesia*

J.F.A. Hendrickx(✉) and A. De Wolf

Safe anesthesia requires the dedicated attention to the patient by a safe anesthesiologist no matter which method, device, or kind of apparatus is in vogue.
Lucien Morris, inventor of the copper kettle (Morris 1994)

Abstract Recent interest in the use of low-flow or closed circuit anesthesia has rekindled interest in the pharmacokinetics of inhaled anesthetics. The kinetic properties of inhaled anesthetics are most often modeled by physiologic models because of the abundant information that is available on tissue solubilities and organ perfusion. These models are intuitively attractive because they can be easily understood in terms of the underlying anatomy and physiology. The use of classical compartment modeling, on the other hand, allows modeling of data that are routinely available to the anesthesiologist, and eliminates the need to account for every possible confounding factor at each step of the partial pressure cascade of potent inhaled agents. Concepts used to describe IV kinetics can readily be applied to inhaled agents (e.g., context-sensitive half-time and effect site concentrations).

J.F.A. Hendrickx
Department of Anesthesiology and Intensive Care, OLV Hospital, Moorselbaan 164, 9300 Aalst, Belgium
jcnwahendrickx@yahoo.com

*Parts of this chapter appeared in Dr. Jan Hendrickx's doctoral thesis (Hendrickx 2004).

J. Schüttler and H. Schwilden (eds.) *Modern Anesthetics.*
Handbook of Experimental Pharmacology 182.

The interpretation of the F_A/F_I vs time curve is expanded by reintroducing the concept of the general anesthetic equation—the focus is shifted from "how F_A approaches F_I" to "what combination of delivered concentration and fresh gas flow (FGF) can be used to attain the desired F_A." When the desired F_A is maintained with a FGF that is lower than minute ventilation, rebreathing causes a discrepancy between the concentration delivered by the anesthesia machine (=selected by the anesthesiologist on the vaporizer, F_D) and that inspired by the patient. This F_D–F_I discrepancy may be perceived as "lack of control" and has been the rationale to use a high FGF to ensure the delivered matched the inspired concentration. Also, with low FGF there is larger variability in F_D because of interpatient variability in uptake. The F_D–F_I discrepancy increases with lower FGF because of more rebreathing, and as a consequence the uptake pattern *seems* to be more reflected in the F_D required to keep F_A constant. The clinical implication for the anesthesiologist is that with high FGF few F_D adjustments have to be made, while with a low FGF F_D has to be adjusted according to a pattern that follows the decreasing uptake pattern in the body. The ability to model and predict the uptake pattern of the individual patient and the resulting kinetics in a circle system could therefore help guide the anesthesiologist in the use of low-flow anesthesia with conventional anesthesia machines. Several authors have developed model-based low FGF administration schedules, but biologic variability limits the performance of any model, and therefore end-expired gas analysis is obligatory. Because some fine-tuning based on end-expired gas analysis will always be needed, some clinicians may not be inclined to use very low FGF in a busy operating room, considering the perceived increase in complexity. This practice may be facilitated by the development of anesthesia machines that use closed circuit anesthesia (CCA) with end-expired feedback control—they "black box" these issues (see Chapter 21).

In this chapter, we first explore how and why the kinetic properties of intravenous and inhaled anesthetics have been modeled differently. Next, we will review the method most commonly used to describe the kinetics of inhaled agents, the F_A/F_I vs time curve that describes how the alveolar (F_A) approaches the inspired (F_I) fraction (in the gas phase, either "fraction," "concentration," or "partial pressure" can be used). Finally, we will reintroduce the concept of the general anesthetic equation to explain why the use of low-flow or closed circuit anesthesia has rekindled interest in the modeling of pharmacokinetics of inhaled anesthetics. Clinical applications of some of these models are reviewed. A basic understanding of the circle system is required, and will be provided in the introduction.

1 Introduction: Nuts and Bolts of the Circle System

The circle system is the anesthesia breathing system most widely used with adults. The kinetic properties of inhaled vapors and carrier gases are significantly affected by the manner in which the anesthesiologist uses the system. A sound understanding

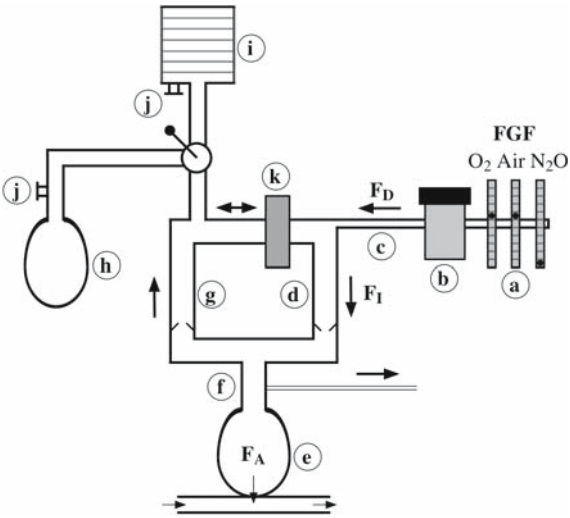

Fig. 1 Nuts and bolts of the circle system

of its composition is essential to understand the remainder of this chapter. We describe the circle system (Fig. 1) by following gases and vapors along their partial pressure cascade. The fresh gas flow rate (FGF) of a carrier gas or gases (O_2, N_2O, and/or air) is selected by adjusting the knobs of the rotameter(s) (Fig. 1, part a). By turning the wheel of the vaporizer (Fig. 1, part b) of the agent of choice, the appropriate amount of anesthetic vapor is added. The concentration of gases and vapors entering the circle system via the common gas outlet (Fig. 1, part c) is referred to as the delivered concentration (F_D). Once these gases enter the inspiratory limb (Fig. 1, part d) they are labeled "inspired mixture" (with concentrations F_I). The composition of the mixture may match that of the delivered gas F_D, or it may be a mixture of delivered gas and some gas that is returning from the previously exhaled tidal volume(s) (see the next section). During inspiration, gases enter the lungs (Fig. 1, part e) from where they are taken up by the body (during wash-in and maintenance). The composition of the exhaled gas is a complex mixture of alveolar gas (F_A) and dead space gas (F_I, since by definition no gas exchange has occurred), and the correct term to describe its concentration is the mixed-expired concentration. Anesthesiologists measure the end-expired or end-tidal concentration, which is the concentration of anesthetic gas in the alveolar part of the exhaled gas, F_A. The sampling port of the gas analyzer is located at the Y-piece (Fig. 1, part f) connecting the circle system to the patient's airway. Exhaled gas then moves along the expiratory limb (Fig. 1, part g) toward either the breathing bag (Fig. 1, part h) when the patient is breathing spontaneously, or toward the bellows of the ventilator (Fig. 1, part i) when ventilation is controlled. Once the breathing bag or the bellows are full, the remainder of the gas still flowing through the expiratory limb is vented to the atmosphere (Fig. 1, part j).

Only when the precise amount of gas and vapor that is being administered is taken up by the patient and/or is lost via leaks and sampling (closed-circuit anesthesia, CCA) will no excess gas be vented. If FGF is higher than minute ventilation, the bag or bellows will be filled with fresh gas only, and all the gas coming from the expiratory limb of the circle system will be vented. However, if FGF is lower than minute ventilation, the bag or bellows will fill with a mixture of fresh gas and exhaled gas coming form the expiratory limb—exhaled gas will therefore be reinhaled or rebreathed. Before reaching the inspiratory limb, rebreathed gases pass though a CO_2 absorber (Fig. 1, part k) to avoid rebreathing of CO_2. With rebreathing, the composition of the inspired mixture (F_I) will differ from the F_D selected by the anesthesiologist.

2 How and Why Kinetics of Intravenous and Inhaled Anesthetics Have Been Modeled Differently

During general anesthesia, the goal of an anesthesiologist is to attain and maintain those concentrations of anesthetic drugs in the blood (and ultimately the effect site) to ensure hypnosis and immobility (suppression of movement after noxious stimulation) (Eger and Sonner 2006). Kinetic models attempt to describe and predict these concentrations, and can be broadly categorized as either physiologic or classic compartmental ("empiric"). With a physiologic model the investigator incorporates the underlying physiologic processes that may affect drug kinetics into the model—the model describes the data as well as the processes by which the observations came to be. With the empiric approach, the only goal is to describe the data.

Because blood concentrations of intravenous anesthetics cannot be measured continuously in the operating room, kinetic models are very useful to optimize maintenance of the desired blood concentration; kinetic models are incorporated in the software that steers syringe pumps (target-controlled infusion, TCI). Pharmacokinetic models for intravenous agents have most often been built empirically because frequently not enough information is available to build physiologic models. Programs like NONMEM fit (multi)exponential curves to the course of the concentrations of the agent of interest using dose history and covariates (e.g., age, gender, weight) as inputs (NONMEM Project Group 1992). The parameters of the model equations are intuitively most accessible when they are expressed as volumes of distributions and clearances because they have a physiologic flavor to it. Nevertheless, these volumes of distribution and clearances are fictitious entities that are not directly related to any underlying anatomic compartments or physiologic processes. The model most often consists of one central and one or two peripheral compartments. The concentration in the central compartment (which matches the blood concentrations which the model predicts) is considered to be the result of drug input into and elimination from a central compartment and drug transfer between compartments (distribution). After the model is derived, it is prospectively tested in a *different* group of patients using performance criteria such as those

developed by Varvel et al.—performance error (PE), median PE (MDPE), median absolute PE, (MDAPE), divergence, and wobble (Varvel et al. 1992). The kinetic models can be incorporated into more complex pharmacokinetic/pharmacodynamic (PK/PD) models that use the effect site concentration to link blood concentrations to a desired clinical end-point, e.g., an EEG derivative such as Bispectral Index (BIS; Aspect Medical Systems, Norwood, MA) when the end-point is hypnosis, or the degree of neuromuscular blockade when muscle relaxants are used. These models can be incorporated in closed-loop systems.

If enough physiologic information *is* available (such as tissue solubilities, tissue volumes, and perfusion), a physiologic model can also be used to describe the kinetics of intravenous agents. For example, a physiologic model predicted lidocaine (Benowitz et al. 1974) and propofol (Levitt and Schnider 2005) plasma concentrations well. The latter study is one of the few quantitative comparisons of physiologic and compartment models available.

The uptake and distribution of inhaled anesthetics have most often been modeled by physiologic models such as Eger's four compartment (4C) model (Eger 1974). Plenty of information is available to build a physiologic model. The parameters needed to calculate the course of tissue partial pressures (tissue volumes, tissue solubilities, and tissue blood flows) can be readily retrieved from the literature (Eger and Saidman 2005). The models assume uptake of anesthetic gases is perfusion limited. Organ vapor capacity depends on the size of the organ and the solubility of the agent in that particular organ. The rate at which the partial pressure in the organ increases, and eventually saturates toward the partial pressure in blood, depends both on the organ's capacity and organ blood flow. This rate is described by a time constant (tissue storage capacity divided by blood flow). Based on both tissue storage capacity and blood flow, Eger grouped organs and tissues into the vessel rich group (VRG), muscle group (MG), fat group (FG), and vessel poor group (VPG) (Eger 1974). Uptake according to the 4C model is presented in Fig. 2, where it is compared with uptake according to the square root of time model (SqRT; see below) and with clinical uptake data. In Eger's five-compartment (5C) model the VRG, MG, and FG from the 4C model are retained; the VPG is deleted because its contribution to uptake is considered insignificant, but a lung and an "intertissue diffusion" compartment are added (Carpenter et al. 1986). The intertissue diffusion group is hypothesized to be fat adjacent to well-perfused tissues. The model has recently been reviewed by Eger and Saidman (2005). The SqRT model was developed by Lowe and Ernst specifically to facilitate the practice of CCA in an era when multigas analyzers were not available (Lowe and Ernst 1981). The sum of uptake by the individual organs was found to increase according to the square root of time, an observation first made by Severinghaus for N_2O (Severinghaus 1954). When the arterial concentration is maintained, the same amount of agent is taken up by the tissues during each subsequent "square root of time" interval (0–1 min, 1–4 min, 4–9 min, 9–16 min, etc.). This amount is called the "unit dose," and is calculated based on patient weight. At the start, a "prime dose" is given to prime the circuit, functional residual capacity, and blood pool. Uptake according to the SqRT model is presented in Fig. 2.

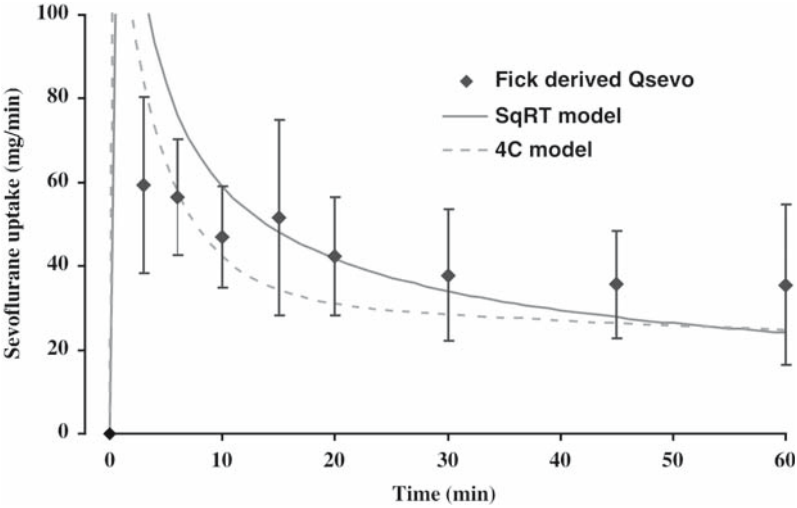

Fig. 2 Comparison of the sevoflurane uptake rate ($mg.min^{-1}$) determined by Fick's method (mean ± standard deviation) with that predicted by the 4C model and the square root of time model (SqRT) model. F_A was maintained at 1.3% (Frietman et al. 2001)

Using modern computer technology, the number of differential equations that can be solved simultaneously is enormous, spurring the development of models with ever-increasing numbers of compartments (Fukui and Smith 1981; Heffernan et al. 1982; Lerou et al. 1991; Vermeulen et al. 1995; Lerou and Booij 2001a). An 18-compartment model by Fukui and Smith (1981), for example, carries over 88 equations and 124 parameter settings. Some of the models simulate how a drug affects its own uptake by, e.g., altering cardiac output (i.e., nonlinear pharmacokinetics).

How complex a model needs to be depends on the goal of the investigator. The more complex models should only be used if they better represent what actually happens or when more sophistication is required, such as when there is the need to study the effect of changes in physiologic parameters on uptake (Vermeulen 2000). The 4C model is intuitive and didactic, and is incorporated in GasMan (Med Man Simulations, Chestnut Hill, MA).The SqRT model by Lowe and Ernst is useful to provide dosing guidelines during CCA. Both models tend to overestimate initial uptake and underestimate it after 30–45 min (Fig. 2 ; Hendrickx et al. 1997, 1998a, 2003; Frietman et al. 2001). Interest in Heffernan's 10-compartment model (Heffernan et al. 1982), first described more than 20 years ago, has rekindled recently in a series of studies by Kennedy to help predict concentrations of inhaled anesthetics during reduced FGF (Kennedy et al. 2002) (see Sect. 5). Sophisticated physiologic models offer advantages over simpler models for the study of interactions among ventilation, circulation, and the uptake and distribution of inhaled agents, and provide the basis for training simulators. Especially with the multicompartment physiologic models, it is important "not to be carried away with uncritical enthusiasm, because these models require an

Table 1 Parameters of the classic two-compartment model of inhaled anesthetics derived from inspired and expired tidal volumes and concentrations of desflurane, isoflurane, and sevoflurane in O_2/N_2O by Wissing et al. (2000). The estimated pharmacokinetic variables and extrapolated parameters are given as median and range (in parentheses)

	Isoflurane		Sevoflurane		Desflurane	
k_{12} (min^{-1})	0.158	(0.065–0.583)	0.117	(0.070–0.344)	0.078	(0.029–0.186)
k_{21} (min^{-1})	0.007	(0.001–0.014)	0.007	(0.001–0.019)	0.011	(0.003–0.022)
Cl_{12} ($ml_{vapor} kg^{-1} min^{-1}$)	30.7	(15.9–38.7)	13	(9.8–22.4)	7	(4.4–11.1)
V_1 ($ml_{vapor} kg_{bw}^{-1}$)	196	(37–332)	106	(57–171)	75	(49–140)
V_2 ($ml_{vapor} kg_{bw}^{-1}$)	4,112	(1,472–9,396)	1,634	(762–8,842)	612	(343–1,850)
V_{ss} ($ml_{vapor} kg_{bw}^{-1}$)	4,285	(1,509–9,640)	1,748	(819–8,997)	698	(408–1,917)

Cl_{12}, transport clearance from central to peripheral compartment; k_{12}, microconstant for transport from central to peripheral compartment; k_{21}, microconstant for transport from peripheral to central compartment; V_1, volume of distribution of the central compartment; V_2, volume of distribution of the peripheral compartment; V_{ss}, volume of distribution during steady state. V_1, V_2, and V_{ss} are given as milliliters of inhaled anesthetic in relation to body weight

immense amount of detailed information, much of which must be assumed, estimated, or simply guessed" (Hull 1997). Even with simple physiologic models many assumptions are made (Hendrickx et al. 1997). Tissue solubilities vary up to 150% between authors (Yasuda et al. 1989), and the tissue homogenates used to determine these coefficients may not represent in vivo conditions. Arterial to end-expired gradients exist that may not be explained by ventilation/perfusion mismatching alone (Landon et al. 1993; Doolette et al. 1998; Doolette et al. 2001). Brain time constants in vivo may be longer than the theoretically calculated values (Lockhart et al. 1991). In addition, from a more practical point, physiologic models are not well suited for the analysis of the F_A vs time curves that are available in a clinical setting (Bouillon and Shafer 2000). One of the strengths of classic compartment modeling is that it can be used without having to take into account these confounding factors, and that they are well suited for the analysis of the F_A vs time curves. Wissing describes classic compartmental parameters for isoflurane, sevoflurane, and desflurane based on inspired and expired concentrations and tidal volumes (Table 1; Rietbrock et al. 2000; Wissing et al. 2000). Yasuda et al. also used classic compartment modeling to describe the kinetics of inhaled anesthetics (Yasuda et al. 1991a, b). The exhaled concentrations of sevoflurane, desflurane, isoflurane, and halothane were measured using chromatography up to a week after these agents had been concomitantly administered for 30 min, and a five-compartment model was derived. In more recent work, arterial and mixed venous blood concentration profiles were linked to uptake derived from inspired and expired tidal volumes and partial pressures using compartment modeling (Ishibashi et al. 2006). Using lung uptake as the input function, the time course profiles of the arterial and the mixed venous blood concentrations were best described by a two- and one-compartment model, respectively. The use of compartment modeling of inhaled agents is currently being applied to derive dosing guidelines for the liquid infusion rate of sevoflurane with a commercially available device AnaConDa® (Hudson RCI, Upplands Väsby, Sweden) (Enlund et al. 2006).

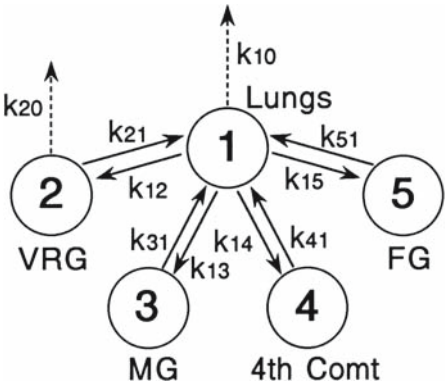

Fig. 3 Five-compartment model derived from end-expired wash-out data (Yasuda et al. 1991a, b)

Can distribution volumes and clearances, the parameters of compartment models, be interpreted in terms of tissue volumes and blood flows? Yasuda et al. (1991a, b; see above) tried to relate the distribution volumes and clearances with tissue volumes and tissue blood flows of a physiologic model. Thus, the first, second, third, fourth, and fifth compartment were interpreted as representing lungs, VRG, MG, intertissue diffusion, and the FG (Fig. 3). In a model developed by Ishibashi et al. (2006) that links arterial and mixed venous blood concentrations to uptake derived from inspired and expired tidal volumes and partial pressures, the relationship between distribution volumes and clearances (the parameters of compartment models) and covariates cardiac output and patient demographic data was not a straightforward one, suggesting that correlating clearances and distribution volumes with tissue volumes and blood flows should be done with care, if at all. Hull also argues that "[while] it is often suggested that some particular tissue or organ (such as the brain) be 'in' one compartment or another, such suggestions are ill-founded because parameters of the fit to the uptake data contain no information that might support such assumptions" (Hull 1997; Shafer 1998). Similarly, Wissing argues that a precise allocation of several hypothetical peripheral compartments to anatomically defined tissues is hardly feasible (Rietbrock et al. 2000). In a theoretical analysis, we documented that both classic compartment modeling and physiologic modeling describe the course of the anesthetic concentrations equally well, but the relationship between the parameters of the two models was complex (Hendrickx et al. 2006a). However, because both physiologic and compartment modeling described the course of the anesthetic concentrations equally well, concepts applied to IV anesthetics such as context-sensitive half-times (Bailey 1997; Eger and Shafer 2005) or k_{eo} (the plasma-effect site equilibration rate constant; Kennedy 2005) can equally well be applied to inhaled agents.

In contrast to the clinical requirement for kinetic models when a specific target concentration of an intravenous agent is aimed for, some authors have suggested that there is no clinical need for kinetic models of potent inhaled anesthetics

(Vermeulen 2000). First, F_A can be continuously measured. Second, F_A defines the concentrations needed to ensure the relevant clinical endpoints of hypnosis and immobility (mediated at the spinal and supraspinal level respectively) through the concepts of MAC_{awake} and MAC (Eger et al. 1965; Stoelting et al. 1970). This dose-response curve for suppression of movement and hypnosis is steep—within a population, MAC varies by not more than 10%–15% among individuals (Sani and Shafer 2003; de Jong and Eger 1975; Eger et al. 2001). Third, the partial pressure in the brain lags behind that in the alveoli with only a modest delay for modern agents—the equilibration half-time of this process (determined using EEG power spectrum) is 2.4 min for isoflurane and sevoflurane and 1.1 min for desflurane (Rehberg et al. 1999). We would therefore argue that the MAC and MAC_{awake} concepts by definition make any kinetic model for inhaled agents also a PK/PD model for the end-points immobility and hypnosis. Some authors prefer to incorporate this delay in their model by introducing an effect site concentration in their model (see Sect. 5) (Kennedy 2005). And finally, automated closed-loop administration of inhaled agents has now enabled the anesthesiologist to select an F_A without having to bother about uptake or delivered or inspired partial pressure to achieve that particular F_A (see Chapter 21). While we concur that inhaled anesthetics can be and are being administered safely without the use of any model, we will show in the remainder of this chapter that models remain of clinical value. Models can help the interested anesthesiologist understand the kinetics of inhaled anesthetics at reduced FGF and thus help him or her to comfortably use inhaled agents and carrier gases with FGF well below 1 l/min. Models are used to develop low-flow administration schedules, in particular to minimize the duration of the high FGF period at the beginning of anesthetic administration that increases anesthetic waste and thus cost and pollution. Models are used to build open loop control systems (Kennedy et al., see Sect. 5) and provide dosage guidelines for the rare CCA enthusiast and for a new liquid agent injection device, the AnaConDa® (Sedana Medical, Sundyberg, Sweden) (Enlund et al. 2006; Enlund et al. 2002). To examine how uptake models can help us better understand the kinetics of inhaled agents in a circle system during low-flow anesthesia, we will first have to expand our interpretation of the F_A/F_I curve.

3 Expanding the Interpretation of the F_A/F_I Curve

F_A/F_I curves that describe how F_A approaches F_I over time (Fig. 4) are widely used to describe the kinetics of inhaled agents in the clinical setting, and have been proven to be of great didactic value to introduce the novice to "uptake and distribution" of inhaled anesthetics (Eger 2000). To correctly interpret the F_A/F_I curve, it is important to understand that these curves do not present actual uptake by the patient. Also, it is important to realize that high FGF and fixed F_I are used (high FGF with constant F_I technique). At a time when no end-expired gas analysis existed and when the introduction of the plenum vaporizer for the first time allowed reasonable control of F_D, a high FGF with constant F_I technique was extremely useful

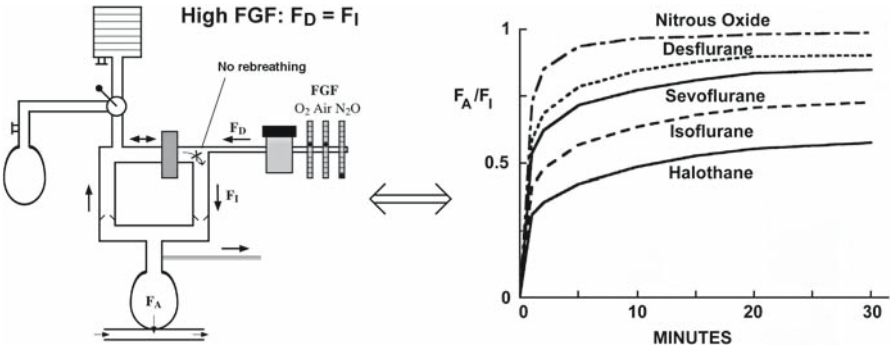

Fig. 4 The interpretation of the F_A/F_I curve when using a circle system requires the understanding that a fixed F_I and a total FGF larger than alveolar ventilation are used (high FGF with constant F_I technique). Under these circumstances, $F_D = F_I$

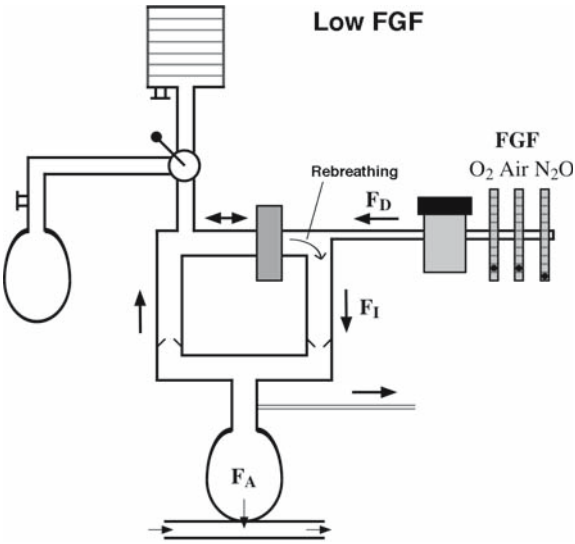

Fig. 5 The circle system and low-flow anesthesia. When FGF is lower than minute ventilation, there will be rebreathing. The lower FGF, the more rebreathing there is, and the larger the discrepancy between F_I and F_D will be

and safe because it ensured F_I matched F_D ($F_D=F_I$) by avoiding rebreathing. What really is implied when the term "high" FGF is used, is that FGF is higher than alveolar minute ventilation. Let us consider what happens when an inhaled agent is administered to a patient via a circle breathing system of an anesthesia machine with standing bellows when FGF is lower than minute ventilation (Fig. 5). Let us assume ventilation is mechanically controlled. Whenever FGF becomes lower than

minute ventilation, FGF alone does not suffice to provide the tidal volume: the ventilator bellows will fill with a mixture of fresh gas and exhaled gas. With the next delivered tidal volume, some of the exhaled gas will thus be inhaled: this is called "rebreathing." The lower FGF, the more rebreathing there is. The rebreathing process is complex, and its effect on the kinetics of vapors depends, on a number of factors, e.g., on the type of carrier gas, the relative percentage of dead space and alveolar ventilation, the configuration of the different parts of the anesthesia circuit, and the location of any leaks. For our purposes, we will only consider the effect of the composition of gas mixture contained in the expired tidal volume. The gas contained in the exhaled tidal volume is not a homogeneous mixture. The first part of tidal volume (about one-third) contains gas that has not participated in gas exchange (dead space ventilation), and will not alter the composition of the inspired mixture to any significant degree when rebreathed because its vapor concentration equals F_I. Next comes alveolar gas, the vapor content of which has been altered by uptake (and all other factors involved in gas exchange across the alveolar–capillary membrane). Overall, the lower the FGF the larger the contribution that the alveolar gas with the lower vapor concentration (F_A) will make to the inspired mixture, leading to a decrease in F_I. To maintain F_I and thus F_A, F_D will have to be increased: a discrepancy has developed between F_D (controlled by the anesthesiologist) and F_I. This discrepancy that has developed between F_D and F_I may be perceived as "lack of control." For this very good reason, anesthesiologists have tended to deliver a fixed inspired partial pressure with a high FGF and watched F_A approach F_I over time. F_A/F_I graphs, discussed extensively by Eger, do graphically explain this process, as well as the effect of ventilation, cardiac output, shunting, and blood/gas partition coefficients (Fig. 6a). The amount of uptake and uptake models themselves are not directly reflected in those graphs—uptake is actually better approximated by the area *above* the F_A/F_I curve, $1\text{-}F_A/F_I$ (Fig. 7; Lin 1994). Still, $1\text{-}F_A/F_I$ is only an approximation of uptake—uptake is the difference between the amount entering and leaving the lungs, and thus has to take inspired and expired volumes into account.

The absence of end-expired gas analysis until the 1980s in most operating rooms did not prevent a few enthusiasts from using FGF well below minute ventilation, down to CCA, where the amount of agent and carrier gases added to the circuit matches the amount taken up by the patient (and lost via leaks) (Lowe and Ernst 1981). The extreme of low FGF, CCA, best illustrates why modeling of uptake became of real interest from a clinical point of view at a time when end-expired gas analysis was not routinely available: knowing the uptake at a certain F_A allowed the anesthesiologist to have a reasonable estimate of the amount of vapor that had to be added to the circuit to maintain the desired (unmeasured) F_A during CCA, because if the amount of vapor added to the circuit equals that removed from it, the concentration of the vapor in the system will remain constant (Lowe and Ernst 1981). The analogy between CCA and intravenous anesthesia is clear: in both cases, models are used to help quantitate the administration of the amount of drug in such a way that the resulting concentration falls within a desired range of concentrations. For inhaled agents, the mass balance also has to take into account the effect of gas sampling, circuit leaks, and circuit absorption. To make the link to a more quantitative

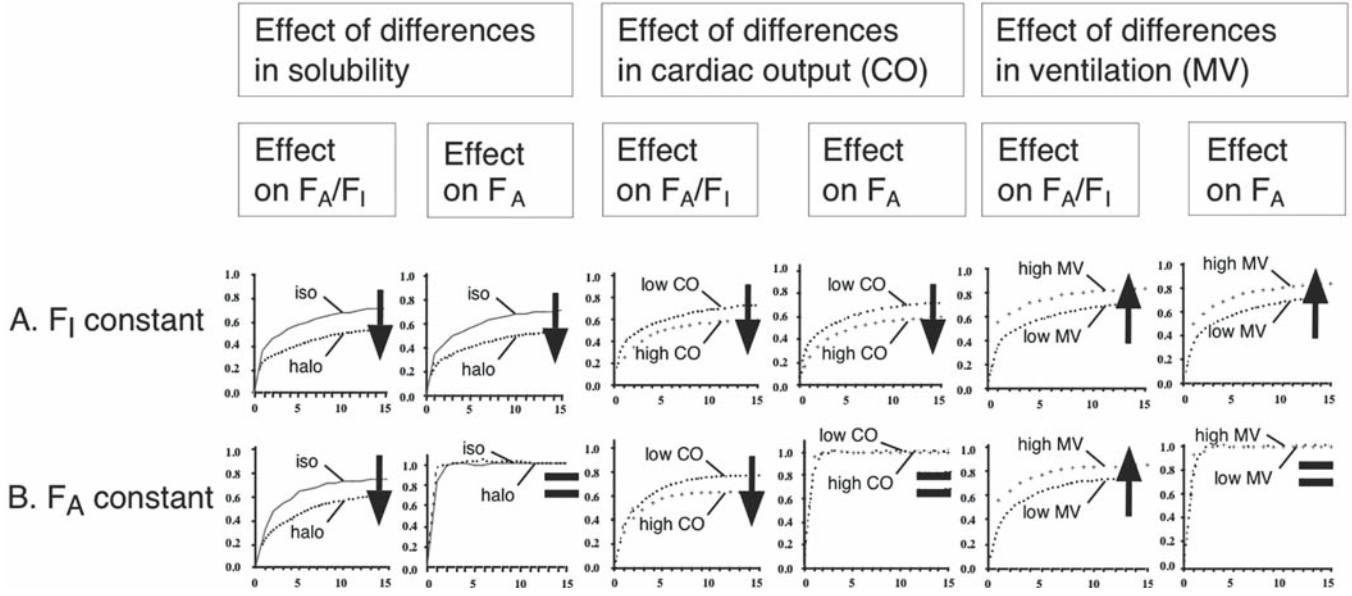

Fig. 6a, b GasMan simulations of how the mode of administration of a potent inhaled agent alters the interpretation of the isoflurane F_A/F_I curve. The qualitative effects on the F_A/F_I curve of an increase in blood/gas solubility (isoflurane vs halothane), cardiac output, and ventilation are the same regardless of whether F_I (**a**) or F_A (**b**) is the controlled variable that is kept constant. However, when F_A is kept constant, differences in solubility, cardiac output, and ventilation will not affect F_A because F_I is adjusted to maintain F_A at the desired concentration

approach to the kinetics of inhaled agents, a slightly different approach than the use of the F_A/F_I curve imposes itself: instead of dialing a constant F_D with high FGF and studying the resulting F_A/F_I curve, the anesthesiologist wonders how a certain desired F_A can be attained and maintained in the individual patient by adjusting F_D, and how this is affected by the FGF selected by the anesthesiologist. We will answer these questions by a clinical example (Hendrickx et al. 1998b; Hendrickx 2004): How does the sevoflurane vaporizer setting have to be adjusted to rapidly attain and maintain the F_A at 1.3% sevoflurane with seven different FGF (8, 4, 2, 1, 0.5, 0.3, and 0.2 l/min, all in O_2/N_2O except the 0.2 l/min group in which O_2 was the carrier gas), starting with the maximum vaporizer setting of 8%? Two important points need to be made before analyzing the example. First, we focus on differences between F_D, F_I, and F_A here (F_D-F_A, F_D-F_I, F_I-F_A) rather than their ratios (F_D/F_A, F_D/F_I, F_I/F_A) because this better explains the existing gradients, and because anesthesiologists administer and measure absolute concentrations rather than ratios. Second, F_A and F_I are not presented because they (predictably) will be the same in all FGF groups by design. At the same (constant) F_A, average patient uptake in the different FGF groups logically will be very similar. Uptake can be approximated by the difference between the amount entering (inspired *alveolar* volume×F_I) and leaving the lung (expired *alveolar* volume×F_A; Fig. 7). Ignoring small differences between inspired and expired alveolar minute ventilation, it thus follows that F_I-F_A equals uptake/alveolar minute ventilation. Because F_A, uptake, and alveolar minute ventilation are the same in all FGF groups, it follows that F_I has to be very similar in all FGF groups at the same point in time. Also note that when uptake (and thus F_I-F_A) is constant, at any point in time a constant F_D-F_I implies that F_D-F_A is also constant.

Figure 8 displays the required vaporizer settings for the above example (Hendrickx et al. 1998b; Hendrickx 2004). Each line represents the mean of settings in 8 patients.

Several important findings on the F_D graph deserve mention.

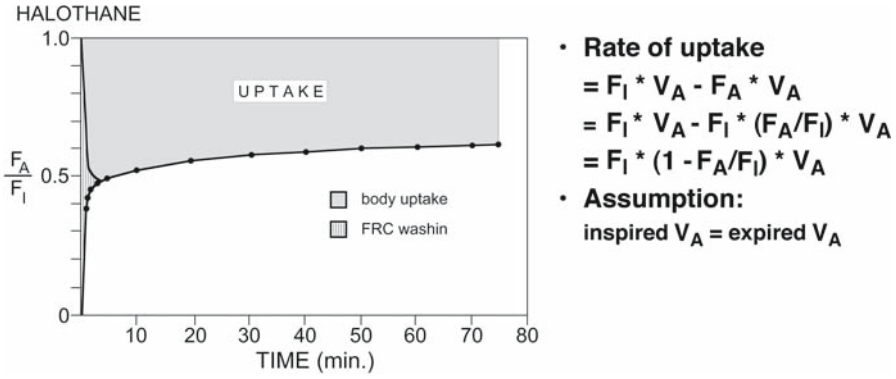

Fig. 7 Uptake is not represented by F_A/F_I itself, but rather by the area above the F_A/F_I curve, called "fraction of uptake" or $1-F_A/F_I$. Rate of uptake=$(1-F_A/F_I)$* alveolar minute ventilation, assuming that inspired and expired alveolar minute ventilation are the same

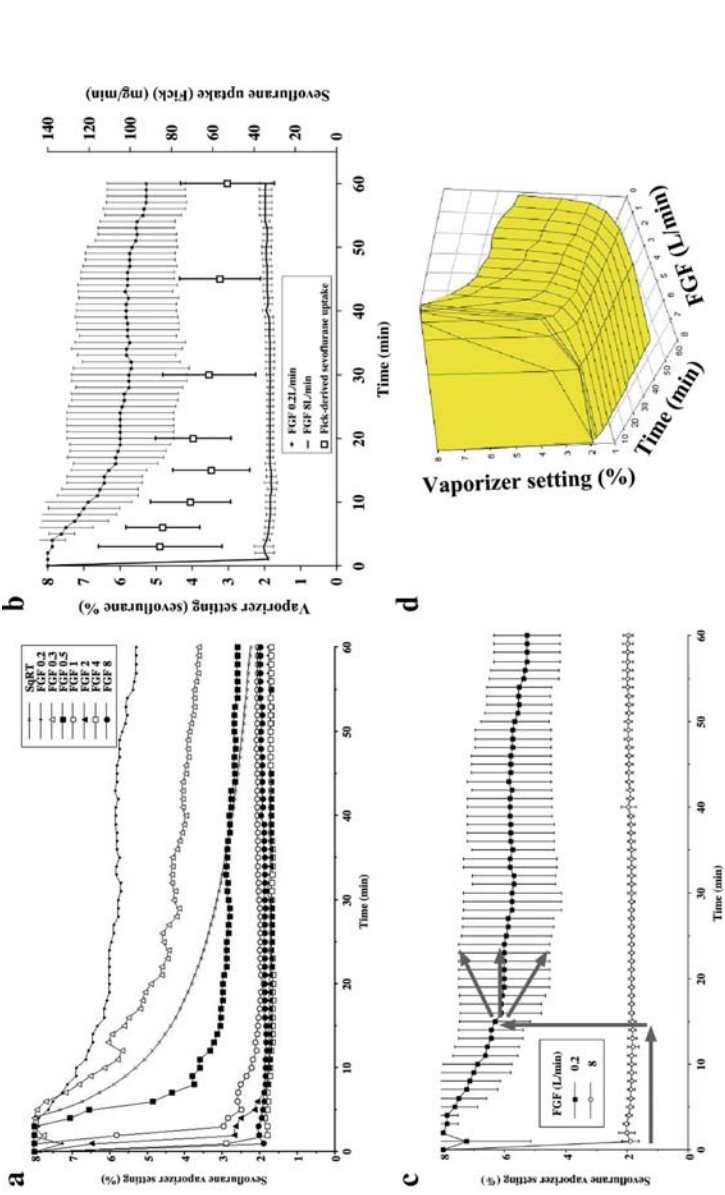

Fig. 8 a Sevoflurane vaporizer setting required to rapidly attain and maintain the F_A at 1.3% sevoflurane with seven different FGF (8, 4, 2, 1, 0.5. 0.3, and 0.2 l/min^{-1}, all in O_2/N_2O except the 0.2 l/min group (100% O_2) starting with the maximum vaporizer setting of 8%. Values in each FGF group represent mean of 8 patients (Hendrickx et al. 1998b). F_D is larger with lower FGF. F_D predicted by the SqRT model (CCA) is added. **b** Overlay of Fick-derived sevoflurane uptake data (Frietman et al. 2001) and F_D in the 0.2 and 8 l/min FGF groups; *error bars* represent standard deviation. The Fick-derived sevoflurane uptake pattern seems to be reflected better in the vaporizer settings with lower FGF. **c** F_D variability increases with lower FGF because of interpatient variability in uptake of up to 50%. As a result, if the anesthesiologist wants to decrease the FGF from 8 to 0.2 l/min, F_D will range from 4% to 8% (*gray arrows*). **d** The information presented in the 2D graph (**a**) can be displayed in a three-dimensional plot, a visual representation of the so-called "general anesthetic equation" or "anesthetic continuum" of sevoflurane

First, a similar vaporizer setting pattern emerges for each FGF (Fig. 8a). After an initial period (30 s to a few minutes) during which the maximum F_D is used to rapidly wash-in the system, F_D can be rapidly decreased, and a phase follows with a more progressive decline over the next 10–15 min (rapidly saturating tissues). After approximately 15 min, no or only a limited number of further F_D changes are needed during the ensuing 45 min (more slowly saturating tissue groups). For example, at an FGF of 1 l/min, the vaporizer setting to maintain the F_A at 1.3% is not different at 60 min than at 15 min (1.9±0.3% at 15 min and 2.0±0.3 at 60 min).

Second, the lower the FGF, the higher the F_D has to be. Said differently, the difference between F_D and F_I increases when FGF is reduced (Fig. 8a). This is caused by rebreathing.

Third, the uptake pattern of sevoflurane seems to be more reflected in the vaporizer settings with lower FGF. At one extreme of FGF, 0.2 l/min, the F_D course can be seen to match the sevoflurane uptake pattern (Fig. 8b). At the other extreme, 8 l/min FGF (FGF > minute ventilation), the uptake pattern is hardly recognizable in the vaporizer settings; the vaporizer setting is high only during the first few minutes because of wash-in of the system combined with high uptake (that is, the first few minutes of the anesthetic). However, if we were to use a very sensitive gas analyzer and an extremely precise vaporizer, the same decreasing F_D pattern observed in the CCA group could be observed in the high FGF groups. Because the difference between F_D and F_I increases with lower FGF (see previous paragraph), the uptake pattern *seems* to be more reflected in lower FGF groups. Nevertheless, the *clinical* implication is that the anesthesiologist has to make barely any F_D changes with high FGF, while with a very low FGF, F_D has to be adjusted in a pattern that follows the decreasing uptake pattern in the body, especially at the beginning of anesthesia when the anesthesiologist may be occupied with a host of other tasks. The reflection of the uptake pattern in the course of F_I (not shown for reasons mentioned above) will be the same in all FGF groups. The difference between F_I and F_A is caused by patient uptake—this is the same for all FGF groups; the difference between F_D and F_I is caused by rebreathing, and thus differs between FGF groups. When FGF is high, there is no rebreathing, and then F_D=F_I.

Fourth, when the F_D predictions by the SqRT model for CCA are compared to those in 0.2 l/min group, it can be appreciated that the SqRT model will initially overestimate and later underestimate F_D (Fig. 8a). This finding is to be expected because the SqRT model initially overestimates and later underestimates uptake of inhaled agents (Fig. 2; Hendrickx et al. 1997, 1998a, 2003; Frietman et al. 2003a, b): the uptake pattern determines the manner in which the anesthesiologist has to adjust F_D. Findings for the 4C models are analogous (Hendrickx 2004).

Fifth, F_D variability increases with lower FGF (Fig. 8b). The lower the FGF, the more uptake by the patient will influence the composition of the inspiratory mixture and therefore the vaporizer setting. Because uptake differs up to 50% between patients (Hendrickx et al. 1997; Frietman et al. 2001), F_D variability increases accordingly with lower FGF (Table 2; Hendrickx 2004; Hendrickx et al. 1999a). The clinical implications of this finding are important. If the anesthesiologist wants to decrease the FGF from 8 to, e.g., 0.2 or 0.3 l/min (Fig. 8c), the F_D for the individual

Table 2 Coefficient of variation of F_D (100×standard deviation/mean) for modern inhaled agents after maintaining 0.65 MAC for 40 min with a range of FGF (Hendrickx 2004; Hendrickx et al. 1999a)

		FGF (l/min)					
Time	Agent	0.3	0.5	1	2	4	8
40 min	Isoflurane	24	12	21	13	10	13
	Sevoflurane	30	19	15	10	3	13
	Desflurane	17	16	6	5	5	6

patient has to be increased to a number that can be anywhere from 4% to 8%, quite a large range. Because patient demographic parameters (e.g., weight) could not be withheld as covariates in most closed-circuit anesthesia studies (Hendrickx et al. 1997, 1998a, 2003; Vermeulen et al. 1997; Westenskow et al. 1983; Lockwood et al. 1993), these covariates cannot be used to help decide which F_D to use in the individual patient, underscoring the need to always use end-expired gas analysis. Even with the application of simple administration schedules (see Sect. 5), clinicians may still find the increased discrepancy between F_D and F_I, coupled with the unpredictability caused by the higher F_D variability at the lower FGF, cumbersome to deal with in a busy operating room. Anesthesia machines that use CCA end-expired feedback control provide a practical solution to these issues—they "black box" these issues (see Chapter 21).

Carrier gas composition also affects F_I–F_A and F_D–F_I. When N_2O is used as the carrier gas instead of O_2 or O_2/air, F_A rises faster and higher because of the second gas effect (Hendrickx et al. 2006b; Slock et al. 2003). Because N_2O increases F_A, to maintain the same F_A, the F_D is slightly lower than when O_2 or O_2/air is used. The use of N_2O also has an effect on the mass balances in the circle system: when N_2O is used, the loss from the circle system will be smaller by the amount of N_2O taken up by the patient (Hendrickx et al. 2002). While the effect of this is small at high FGF because the amount of potent inhaled anesthetic lost via the pop-valve is large relative to uptake by the patient, this effect lowers the required F_D at the lower FGF, such as 500 ml/min: at this low FGF, the amount of gas lost via the pop-off valve with a O_2/N_2O mixture is 100–250 ml/min lower than with 100% O_2. To compensate for these higher losses with O_2 at these low FGF, F_D has to be increased (Hendrickx et al. 2002).

4 The General Anesthetic Equation Concept

The information presented in the 2D graph of the pervious section can be displayed in a three-dimensional plot (Fig. 8d). This 3D figure is a visual representation of the so-called "general anesthetic equation" (GAEq) or "anesthetic continuum" of sevoflurane. "General" and "continuum" refer to the fact that an infinite number of combinations of FGF and F_D can be used to attain and maintain the same F_A (Lowe and Ernst 1981). While the graph only presents the F_D for one particular F_A (1.3% sevoflurane), we nevertheless will further refer to it as the "general" anesthetic equation.

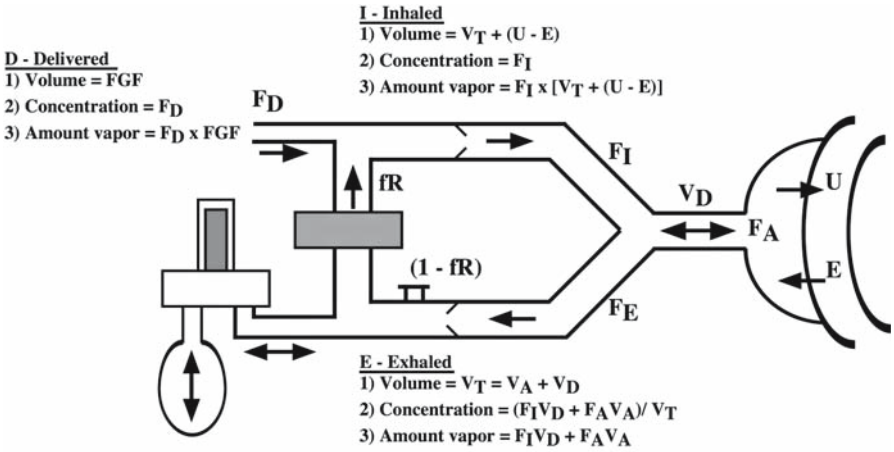

$$F_D = \frac{Qan\,[V_T + (U - E) - V_D \times fR] + (1 - fR)\,F_A \times V_A\,[V_T + (U - E)]}{V_A + (U - E)\,FGF}$$

Fig. 9 Amounts of gases (concentration *x* volume) delivered to the circle system and inhaled and exhaled by the patient. By rearranging these factors Lowe and Ernst derived the general anesthetic equation. F_E, mixed-expired concentration; V_T, V_D, and V_A, minute, dead space, and alveolar minute ventilation, respectively; *U*, uptake of O_2 (VO_2), N_2O (QN_2O), and anesthetic vapor (*Qan*); *E*, elimination of CO_2 (VCO_2) and water vapor (VH_2O); *fR*, fraction rebreathed; *1-fR*, fraction of exhaled vapor exhausted from the system

The word "equation" refers to an actual equation that Lowe and Ernst derived by considering mass balances in the anesthesia system (Fig. 9; Lowe and Ernst 1981). In an extensive treatise, Lowe and Ernst (1981) deduced how the F_D required to attain and maintain a constant F_A in a circle system can be predicted for any FGF if the following are known: (1) uptake of potent inhaled anesthetic, O_2, and N_2O; (2) CO_2 and H_2O production; and (3) alveolar and dead space ventilation. Figure 9 displays those mass balances. The amounts of gases delivered, inhaled, and exhaled can mathematically be quantified. By rearranging the components of these equations, an equation can be derived that mathematically expresses the vaporizer settings over time required to attain and maintain a constant end-expired concentration with a range of FGF: the GAEq (Fig. 9). The equation says that (**1**) F_D is proportional to 1/FGF (F_D–F_I discrepancy increases with lower FGF), (**2**) F_D is proportional to Qan (=uptake; more uptake implies need for higher F_D to maintain F_A), (**3**) and when the factor time is added, ΔF_D is proportional to ΔQan (the uptake pattern or course is reflected in F_D setting over time). Even though many more factors are involved, and a more complex description can be used [incorporating factors such as nitrogen wash-out, physiologic vs anatomical dead-space ventilation, generalization

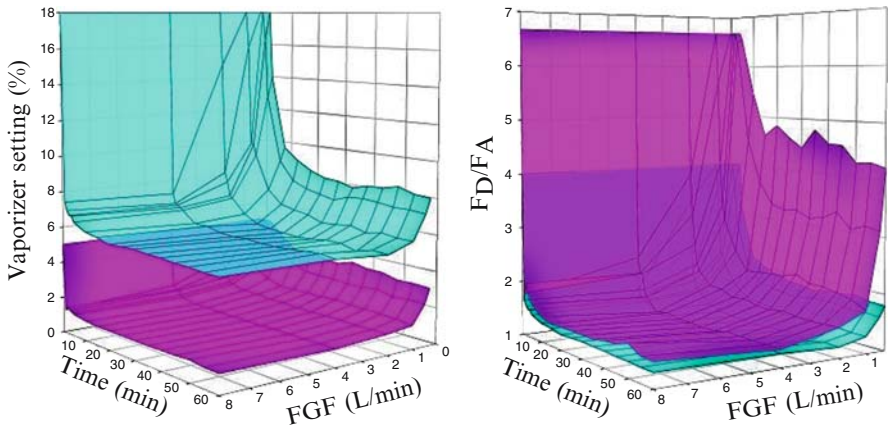

Fig. 10 The 3D representation of the GAEq of 0.65 MAC isoflurane (*purple*) and desflurane (*blue*), with F_D (*left*) and F_D/F_A (*right*) in the Y-axis. While F_D is higher for desflurane because of its higher MAC, the discrepancy between F_D and F_A (or F_D/F_A) is lower for desflurane because of its lower solubility

to STPD (standard temperature and pressure, and dry) conditions, etc.], this concept has didactic value and will help gain insight in how different authors have approached the same "anesthetic plane" from different perspectives.

A 3D plot can be constructed for any F_A with any agent and agent/carrier gas combination (Hendrickx et al. 1998b, c, 1999b; Hendrickx 2004). Figure 10 compares the F_D for isoflurane and desflurane settings to attain and maintain the same MAC (0.65 MAC). The GAEq patterns differ between agents: the agent with the lower blood/gas solubilities (desflurane) has higher absolute F_D because its MAC is higher, but its vaporizer/end-expired ratios (F_D/F_A) are lower than those for isoflurane. The plane for sevoflurane (Fig. 8d) lies between that of isoflurane and desflurane. It has been suggested that the agents with a lower blood/gas partition coefficient would be more "user-friendly" because (1) their F_A/F_I (Fig. 4) is higher (F_A is closer to F_I) and F_D/F_A (Fig. 10) and F_D/F_I are lower—there is less of a discrepancy between the F_D, F_I, and F_A; (2) the more horizontal-shaped plane for desflurane indicates that FGF can be lowered without having to change F_D to a great extent; and (3) vaporizer setting variability is lower with less soluble agents, especially with lower FGF (Table 2; Hendrickx 2004; Hendrickx et al. 1999a).

The plot is also useful to point out how different authors have been studying different parts of the same concept (Fig. 11). From CCA to high FGF one can appreciate the work by Lowe and Ernst (1981; SqRT model, CCA), Virtue (1974; 500 ml/min FGF or minimal flow anesthesia), Foldes et al. (1952; 1 l/min FGF or low-flow anesthesia), and Eger (2000; intermediate- and high-flow regions). Various authors have explored smaller parts of the GAEq, but unfortunately most often using a constant F_D (Johansson et al. 2001, 2002; Park et al. 2005). Nevertheless, the studies by Johansson et al. (2001, 2002) nicely illustrate for both desflurane and sevoflurane

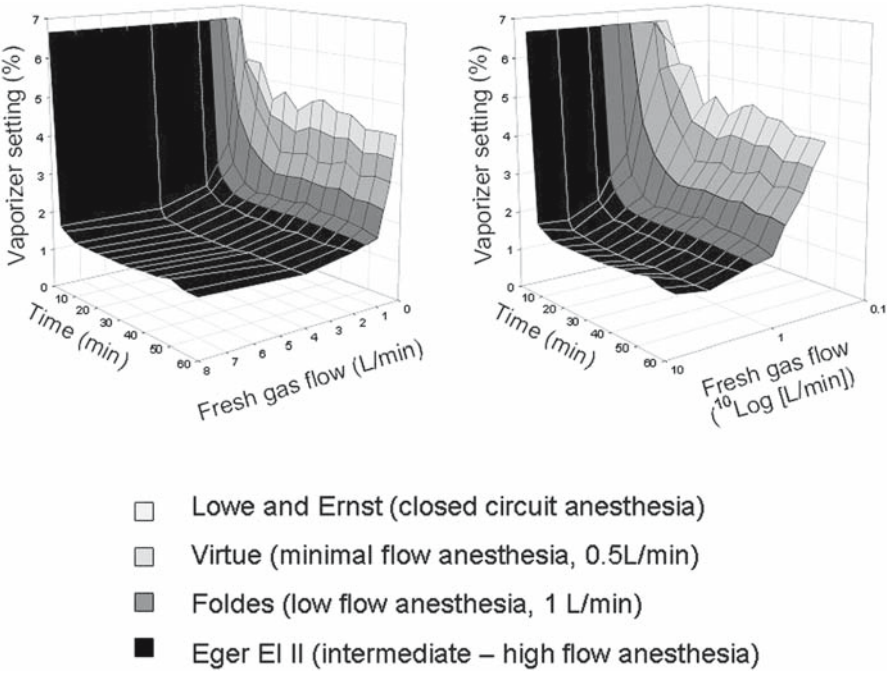

Fig. 11 The 3D plot of the GAEq illustrates how different authors have been studying different parts of the same concept

Table 3 F_A/F_I, F_D/F_I, and F_D/F_I of desflurane and sevoflurane at a FGF of 1 and 2 l/min after 120 min with constant F_D technique (Johansson et al. 2001, 2002)

		Ratios after 120 min of anesthesia with constant F_D		
Agent and carrier gas	FGF (l/min)	F_A/F_I	F_D/F_I	F_D/F_A
Desflurane in O_2/N_2O	1	0.96	1.10	1.14
	2	0.96	1.05	1.09
Sevoflurane in O_2/N_2O	1	0.88	1.38	1.56
	2	0.89	1.22	1.37

how F_A/F_I at 120 min are identical at 1 and 2 l/min FGF, but F_D/F_I and F_D/F_I are higher with the lower FGF (Table 3).

The focus on how to manipulate F_D to attain and maintain a certain F_A when FGF is reduced has implications on how to interpret the effect of cardiac output, ventilation, and solubility on the F_A/F_I curve (Fig. 6). When F_A is kept constant (Fig. 6b), by definition, cardiac output, ventilation, and the use of agents with a different blood/gas partition coefficient will not affect F_A because F_D and thus F_I will be adjusted

to maintain F_A. While the effects of changes in solubility, cardiac output, and ventilation on F_A/F_I are qualitatively similar when either F_I or F_A is kept constant, the effect on the course of F_A and thus tissue partial pressures will be different. The clinical implications remain largely unexplored (Neckebroek et al. 2001; Hendrickx et al. 1999c).

5 The Ideal FGF–F_D Sequence

The GAEq concept suggests that uptake models could be useful to build administration schedules to facilitate the practice of low-flow anesthesia. With high FGF, the model "F_D=constant" may maintain a fairly constant F_A reasonably well after initial wash-in. The lower the FGF, the more accurately the model will have to be to predict the actual uptake by the individual patient because that uptake pattern will be reflected more in the manner in which the anesthesiologist has to adjust F_D compared with the use of higher FGF. Ultimately, performance of even the best model will be limited by interpatient variability in uptake that cannot be accounted for by covariate analysis. Authors have defined the ideal FGF–F_D sequence as the consecutive series of vaporizer and/or FGF settings that allows the anesthesiologist to economically attain and maintain the desired F_A of wanted gases and vapors in a way that remains clinically convenient and avoids or minimizes the presence of unwanted gases (trace gases and, depending on the technique, N_2) (Mapleson 1998). This search can be visualized as finding the optimal route of vaporizer and FGF sequence through a 3D representation of the GAEq (Fig. 12a). The number of

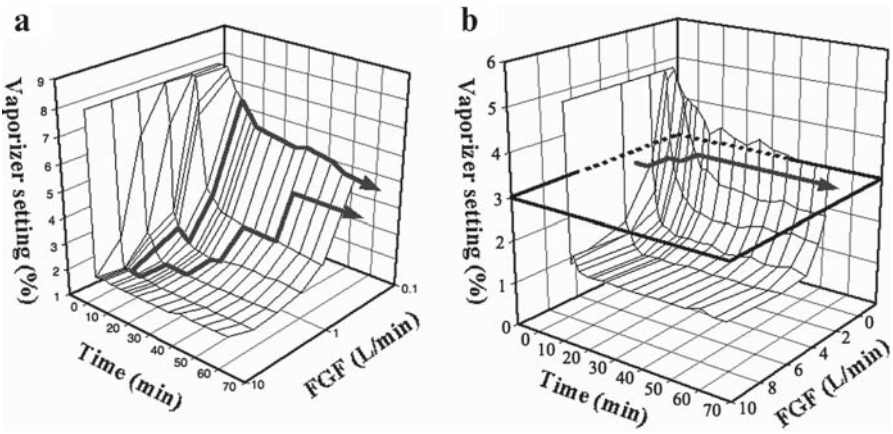

Fig. 12 **a** The search for the ideal FGF–F_D sequence can be visualized as **a** finding the optimal route of vaporizer and FGF sequence through a 3D representation of the GAEq (sevoflurane in this example). **b** The development of a simple low-flow administration schedule for isoflurane in O_2/N_2O with a constant isoflurane F_D by Lerou et al. (Lerou and Booij 2001a, b, 2002; Lerou et al. 2002) can be visualized as the intersection between the plane describing the GAEq for 0.8%–1.1% end-expired isoflurane and the horizontal plane describing a constant vaporizer setting

routes is infinite. Several authors have developed administration schedules but do not explicitly mention the GAEq, yet conceptually they try to approach a certain "path" through this "anesthetic continuum." The attractiveness of the GAEq, and the "planes" or "surfaces" is that they make it clear that in order to keep F_A constant, either FGF or F_D can be adjusted.

When authors search for a "simple" administration schedule, it means "simple to apply but still close enough to the real uptake pattern." Uptake continually changes over time, but because our techniques are crude relative to the uptake changes that actually occur and because these small concentration changes that occur are clinically irrelevant, it may appear as if it does not change during some intervals. Thus, during certain time periods the changes are so small that we can neglect them: This allows us to use "simple" uptake patterns but still be close enough to the real uptake pattern that there is no real penalty to pay for the introduced simplicity.

While the idea of using the uptake pattern to facilitate the administration of inhaled anesthetics is corroborated by other authors (Rietbrock et al. 2000; Lerou et al. 2002), the number of good studies trying to develop these schedules are few, especially those describing strategies to rapidly achieve and maintain a predetermined F_A under low-flow conditions (Lerou et al. 2002). Some of these are reviewed below.

Lowe and Ernst specifically developed the SqRT model to facilitate CCA, yet while mentioning that the 4C physiologic model lacks sufficient clinical validation at the time (Lowe and Ernst 1981), they did not further explore the GAEq clinically themselves. Because their model tends to overestimate initial uptake and thus vaporizer settings, and underestimates them after approximately 30 min (see Fig. 2), it tends to overestimate initial F_D settings and underestimates F_D settings later (Hendrickx 2004).

Mapleson used a multicompartmental physiologic model of the patient and breathing system to predict the ideal FGF sequence at the start of low-flow anesthesia (up to 20 min of anesthesia) using halothane, enflurane, isoflurane, sevoflurane, and desflurane, in a standard male of 40 years old and 70 kg body weight (Mapleson 1998). The goal was to define the FGF and F_D combination that for each anesthetic would raise F_A to 1 MAC as quickly as practically possible and then keep it within ± 5% of that level for 20 min. N_2O was not used. The resulting theoretical combination of FGF and F_D is presented in Fig. 13 (Mapleson 1998). The model has been tested clinically (Ip-Yam et al. 2001; Sobreira et al. 2001): the desired F_A was reached in less than 2 min, but overall mean F_A was at least 10% higher than predicted, and in some instances up to 40%.

Lerou and colleagues' most recent model consists of a physiologic multicompartment model of the body, a three-compartment lung, and a three-compartment breathing system (Lerou and Booij 2001a; Fig. 14). The model meets three criteria: (1) all gases are included, and their partial pressures always add up to 100%; (2) the FGF can range form CCA to higher than minute ventilation; and (3) the breathing system consists of three parts (inspiratory subsystem, sodalime canister, and expiratory tubing plus standing bellows). The model was used to develop a theoretical "ideal FGF and F_D combination schedule" for isoflurane in N_2O. The authors allude to interpatient variability being an issue with the use of a FGF of 0.5 l/min in their

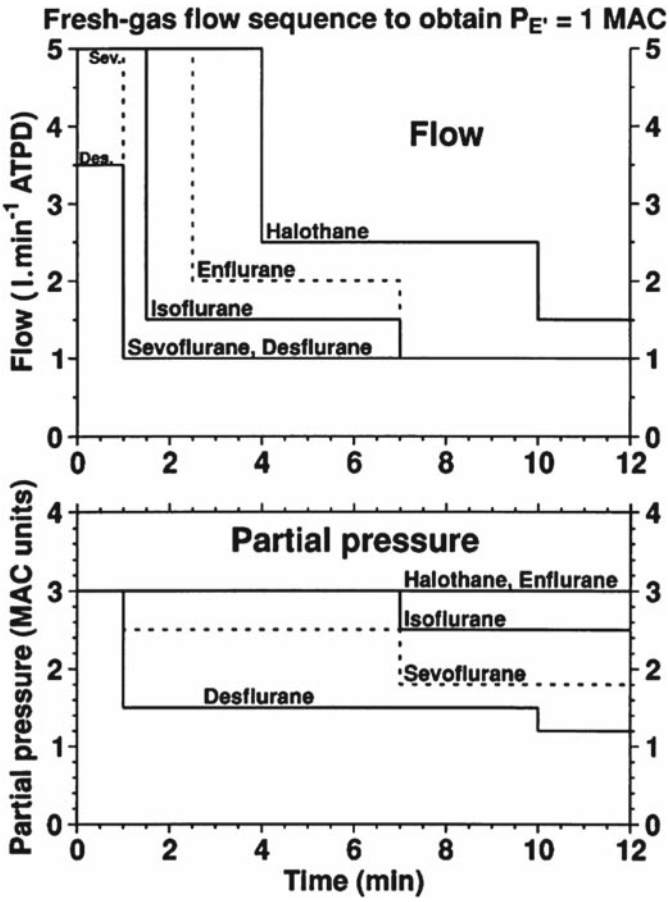

Fig. 13 Theoretical ideal FGF sequence according to Mapleson (1998). Predicted sequence of FGF and partial pressure settings for five anesthetics to achieve and maintain an F_A (labeled $P_{E'}$ here) of 1 MAC using a minimum FGF of 1 l/min

theoretical analysis: the model tends to overshoot for small patients and undershoot in heavier patients (Lerou et al. 2002). The clinically evaluated schedule (Lerou et al. 2002) was started after a 7 to 13 min high O_2/N_2O FGF period without isoflurane, and subsequently consisted of a constant F_D of 3% isoflurane and the following FGF sequence: 2 l/min N_2O+1 l/min O_2 from 0–3 min, 1 l/min N_2O+0.5 l/min from 3–6 min, and 0.2 l/min N_2O+0.3 l/min O_2 after 6 min. Isoflurane F_A reached the desired 0.8%–1.1% range after 2 min (range 1.0–5.67 min), and an average of 72% of individual measurements were within the window from 3–30 min. The approach by Lerou is easy to grasp intuitively if we see their approach in the 3D GAEq graph (Fig. 12b). Lerou describes the intersection between the plane describing the GAEq for 0.8%–1.1% and the plane describing a constant vaporizer setting.

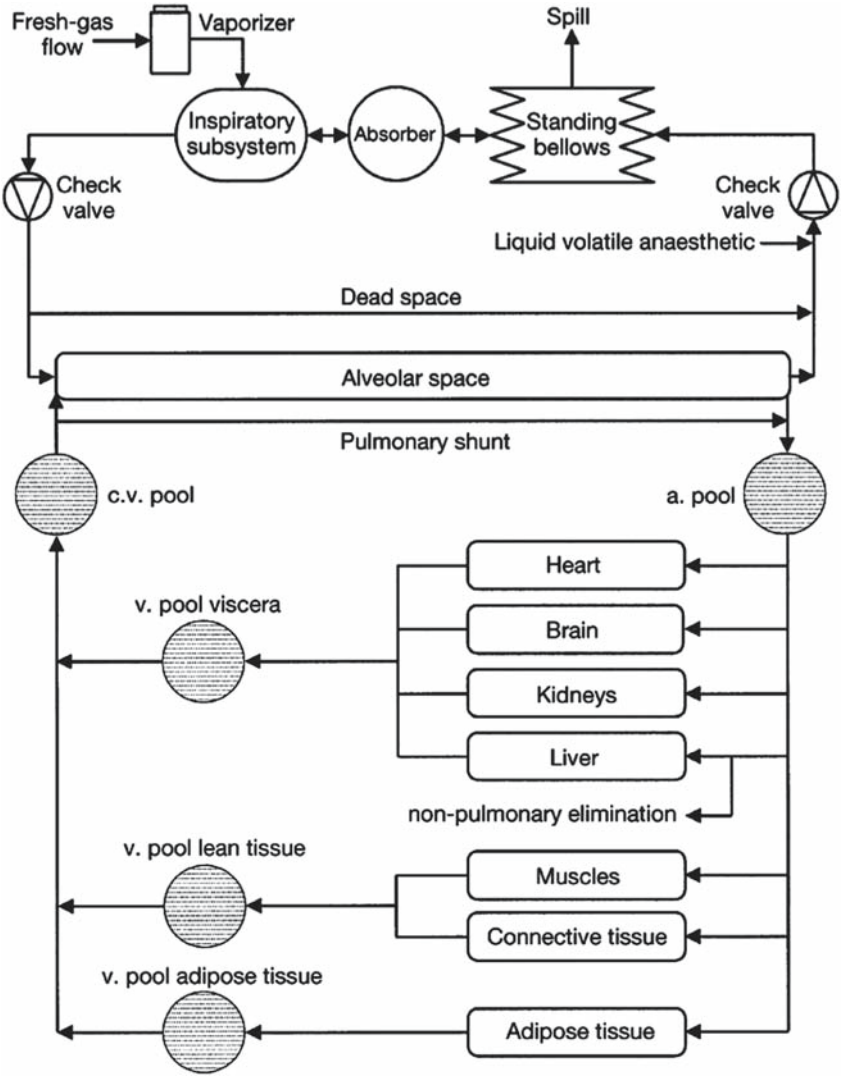

Fig. 14 Diagram of the system model used by Lerou and Booij in their search for a simple low-flow administration schedule for isoflurane in O_2/N_2O (Lerou and Booij 2001a)

Alternative "routes" are obviously possible. We believe administration schedules can be even further optimized and simplified, even with the use of an O_2/N_2O mixture (Carette et al. 2004).

Hendrickx and colleagues did not develop a new model but used the F_D settings from the 1 l/min group in the experiment mentioned section 3 (Hendrickx et al. 1998b; Hendrickx 2004) to develop a simple low-flow anesthesia schedule after overpressure induction (Hendrickx et al. 2000) with sevoflurane (8%) in an 8 l/min O_2/N_2O mixture

for 2.5 min. After a laryngeal mask airway (LMA) was applied, the FGF was lowered to 1 l/min using O_2 and N_2O (0.4/0.6), and the vaporizer was switched off until F_A had decreased to 1.3%, after which it was set at 1.9%. F_A approached 1.3% after 9.0±1.5 min and remained nearly constant during at least 30 min. Clinically derived FGF-F_D data could prove useful to further develop administration schedules.

Ross Kennedy validated a model that incorporates the anesthesia circuit and a nine-compartment physiologic model based on that of Heffernan (itself a modification of Mapleson's model) (Kennedy et al. 2002). FGF, F_D, and F_A data were collected at 10-s intervals during 30 elective anesthetics with either sevoflurane or isoflurane. Control of FGF, F_D, and F_A was left at the discretion of the attending anesthesiologist. FGF, F_D, and F_A were run through a program containing the model. Tissue volumes were scaled linearly to weight, and cardiac output and ventilation calculated according to Brody's formula (Lowe and Ernst 1981). The model predicted F_A well in these patients: MDPE was −0.24%, MDAPE 13.7%, divergence 2.3%/h, and wobble 3.1%. The model was subsequently adapted for use with real-time FGF and F_D data to display a 10-min prediction of the sevoflurane F_A (Kennedy et al. 2004). When the anesthesiologist was instructed to attain a predetermined F_A as rapidly as possible with a FGF of 1 l/min, the predictive display increased the speed to attain the new F_A by a factor 1.5–2.3 times, but there were no differences in the degree of overshoot or stability. The authors argue that these differences are comparable to those seen with an automatic feedback control system, and that the system may simplify the use of low-flow anesthesia. Evaluation of the model's performance with lower FGF is still lacking. The authors are now integrating the effect-site concentration in their predictive display (Kennedy 2005).

6 Compartment Modeling of Sevoflurane Liquid Injection by the AnaConDa®

A new device, the anesthetic conserving device (AnaConDa®), infuses liquid agent via a syringe pump into a device placed at the Y-piece of the breathing circuit where it immediately vaporizes (Enlund et al. 2002; Tempia et al. 2003). Because a large part of the agent is retained in the device upon exhalation and reused during the next inhalation, consumption becomes equivalent to that used with a circle system with a FGF of approximately 1.5 l/min. A population pharmacokinetic model analogous to that used for intravenous agents is being developed for sevoflurane administration with the AnaConDa® (Enlund et al. 2006). The sevoflurane concentration-time courses on the patient side of the AnaConDa® were adequately described with a two-compartment model. The model was capable of handling rapid changes in infusion rate, with a precision of the predictions within ±20.4% MDAPE. MDPE was −2.99%. The authors suggest "the possibility of safe open loop administration of sevoflurane even in the absence of end-expired concentration monitoring" because it can be administered with the "predictive performance of [a] model [that] compares favorably

with that of pharmacokinetic models used for TCI application of intravenous drugs" (Enlund et al. 2006). Further studies will focus on prospective testing and validation of the model implemented in a TCI device, and will define the place of this device in our clinical armamentarium.

References

Bailey JM (1997) Context-sensitive half-times and other decrement times of inhaled anesthetics. Anesth Analg 85:681–686

Benowitz N, Forsyth FP, Melmon KL, Rowland M (1974) Lidocaine disposition kinetics in monkey and man. I. Prediction by a perfusion model. Clin Pharmacol Ther 16:87–98

Bouillon T, Shafer SL (2000) Hot air or full steam ahead? An empirical pharmacokinetic model of potent inhalational agents. Br J Anaesth 84:429–431

Carette R, Hendrickx J, Deloof T, et al (2004) Bellows volume changes associated with very early O_2/N_2O fresh gas flow (FGF) reductions. Anesthesiology 101:A482

Carpenter RL, Eger EI, Johnson BH, et al (1986) Pharmacokinetics of inhaled anesthetics in humans: measurements during and after the simultaneous administration of enflurane, halothane, isoflurane, methoxyflurane, and nitrous oxide. Anesth Analg 65:575–582

de Jong RH, Eger EI (1975) MAC expanded: AD50 and AD95 values of common inhalation anesthetics in man. Anesthesiology 42:384–389

Doolette DJ, Upton RN, Grant C (1998) Diffusion-limited, but not perfusion-limited, compartmental models describe cerebral nitrous oxide kinetics at high and low cerebral blood flows. J Pharmacokinet Biopharm 26:649–672

Doolette DJ, Upton RN, Zheng D (2001) Diffusion-limited tissue equilibration and arteriovenous diffusion shunt describe skeletal muscle nitrous oxide kinetics at high and low blood flows in sheep. Acta Physiol Scand 172:167–177

Eger EI (1974) Anesthetic uptake and action. Williams & Wilkins, Baltimore

Eger EI (2000) Uptake and distribution. In: Miller R (ed) anesthesia, 5th edn. Churchill Livingstone, New York, pp 74–95

Eger EI, Saidman LJ (2005) Illustrations of inhaled anesthetic uptake, including intertissue diffusion to and from fat. Anesth Analg 100:1020–1033

Eger EI, Shafer SL (2005) Tutorial: context-sensitive decrement times for inhaled anesthetics. Anesth Analg 101:688–696

Eger EI, Sonner JM (2006) Anaesthesia defined (gentlemen, this is no humbug). Best Pract Res Clin Anaesthesiol 20:23–29

Eger EI, Saidman LJ, Brandstater B (1965) Minimum alveolar anesthetic concentration: a standard of anesthetic potency. Anesthesiology 26:756–763

Eger EI, Fisher DM, Dilger JP, et al (2001) Relevant concentrations of inhaled anesthetics for in vitro studies of anesthetic mechanisms. Anesthesiology 94:915–921

Enlund M, Lambert H, Wiklund L (2002) The sevoflurane saving capacity of a new anaesthetic agent conserving device compared with a low flow circle system. Acta Anaesthesiol Scand 46:506–511

Enlund M, Kietzmann D, Bouillon T, et al (2006) Population pharmacokinetics of sevoflurane with the AnaConDa®. Towards volatile-TCI. American Society of Anesthesiologists annual meeting abstracts 105:A1569

Foldes FF, Ceravolo AJ, Carpenter SL (1952) The administration of nitrous oxide-oxygen anesthesia in closed systems. Ann Surg 136:978–981

Frietman P, Hendrickx J, Grouls R, et al (2001) Fick-derived sevoflurane uptake. Anesthesiology 95:A478

Frietman P, Hendrickx J, Grouls R, et al (2003a) The correlation between the sevoflurane uptake pattern and vaporizer dial settings at different fresh gas flows. Eur J Anaesthesiol 30:A451

Frietman P, Hendrickx J, Van Zundert A, et al (2003b) Fick-derived Halothane Uptake: a Comparison with the 4C and SqRT Models and with Closed-Circuit Anesthesia Liquid Injection-derived Halothane Uptake. Eur J Anaesthesiol 30:A511

Fukui Y, Smith NT (1981) Interactions among ventilation, the circulation, and the uptake and distribution of halothane—use of a hybrid computer multiple model. I. The basic model. Anesthesiology 54:107–118

Heffernan PB, Gibbs JM, McKinnon AE (1982) Teaching the uptake and distribution of halothane. A computer simulation program. Anaesthesia 37:9–17

Hendrickx J (2004) The pharmacokinetics of inhaled agents and carrier gases. PhD thesis. Faculty of Medicine and Health Sciences, Department of Anesthesiology. University of Ghent

Hendrickx JF, Soetens M, Van der Donck A, et al (1997) Uptake of desflurane and isoflurane during closed-circuit anesthesia with spontaneous and controlled mechanical ventilation. Anesth Analg 84:413–418

Hendrickx JF, Van Zundert AA, De Wolf AM (1998a) Sevoflurane pharmacokinetics: effect of cardiac output. Br J Anaesth 81:495–501

Hendrickx JF, Van Zundert AAJ, De Wolf AM (1998b) Clinical evaluation of the general anesthetic equation for sevoflurane. Anesthesiology 89:A518

Hendrickx JF, Van Zundert A, De Wolf A (1998c) Clinical evaluation of the general anesthetic equation for isoflurane. Anesth Analg 86:S461

Hendrickx JF, Van Zundert A, De Wolf A (1999a) Vaporizer setting variability increases with lower fresh gas flows. Anesth Analg 88:S344

Hendrickx JF, De Ridder KD, De Geyndt AD, et al (1999b) Clinical evaluation of the general anesthetic equation for desflurane. Anesth Analg 88:S341

Hendrickx JF, Van Zundert A, De Wolf A (1999c) Blood/gas solubility and alveolar rate of rise of potent inhaled anesthetics during open-loop feedback administration using a closed-circuit anesthesia liquid injection technique. Anesth Analg 88:S342

Hendrickx JF, Vandeput DM, De Geyndt AM, et al (2000) Maintaining sevoflurane anesthesia during low-flow anesthesia using a single vaporizer setting change after overpressure induction. J Clin Anesth 12:303–307

Hendrickx JF, Coddens J, Callebaut F, et al (2002) Effect of N_2O on sevoflurane vaporizer settings during minimal- and low-flow anesthesia. Anesthesiology 97:400–404

Hendrickx JF, Dishart MK, De Wolf AM (2003) Isoflurane and desflurane uptake during liver resection and transplantation. Anesth Analg 96:356–362

Hendrickx JF, Lemmens HJ, Shafer SL (2006a) Do distribution volumes and clearances relate to tissue volumes and blood flows? A computer simulation. BMC Anesthesiol 6:7

Hendrickx JF, Carette R, Lemmens HJ, De Wolf AM (2006b) Large volume N_2O uptake alone does not explain the second gas effect of N2O on sevoflurane during constant inspired ventilation. Br J Anaesth 96:391–395

Hull C (1997) Pharmacokinetics for anaesthesia, 1st edn. Heinemann, Oxford

Ip-Yam PC, Goh MH, Chan YH, Kong CF (2001) Clinical evaluation of the Mapleson theoretical ideal fresh gas flow sequence at the start of low-flow anaesthesia with isoflurane, sevoflurane and desflurane. Anaesthesia 56:160–164

Ishibashi T, Hendrickx J, De Wolf A, et al (2006) Isoflurane pharmacokinetics: linking lung uptake to arterial and mixed venous blood concentrations. Anesthesiology 105:A1202

Johansson A, Lundberg D, Luttropp HH (2001) Low-flow anaesthesia with desflurane: kinetics during clinical procedures. Eur J Anaesthesiol 18:499–504

Johansson A, Lundberg D, Luttropp HH (2002) The quotient end-tidal/inspired concentration of sevoflurane in a low-flow system. J Clin Anesth 14:267–270

Kennedy RR (2005) The effect of using different values for the effect-site equilibrium half-time on the prediction of effect-site sevoflurane concentration: a simulation study. Anesth Analg 101:1023–1028

Kennedy RR, French RA, Spencer C (2002) Predictive accuracy of a model of volatile anesthetic uptake. Anesth Analg 95:1616–1621
Kennedy RR, French RA, Gilles S (2004) The effect of a model-based predictive display on the control of end-tidal sevoflurane concentrations during low-flow anesthesia. Anesth Analg 99:1159–1163
Landon MJ, Matson AM, Royston BD, et al (1993) Components of the inspiratory-arterial isoflurane partial pressure difference. Br J Anaesth 70:605–611
Lerou JG, Booij LH (2001a) Model-based administration of inhalation anaesthesia. 1. Developing a system model. Br J Anaesth 86:12–28
Lerou JG, Booij LH (2001b) Model-based administration of inhalation anaesthesia. 2. Exploring the system model. Br J Anaesth 86:29–37
Lerou JG, Booij LH (2002) Model-based administration of inhalation anaesthesia. 3. Validating the system model. Br J Anaesth 88:24–37
Lerou JG, Dirksen R, Beneken Kolmer HH, Booij LH (1991) A system model for closed-circuit inhalation anesthesia. I. Computer study. Anesthesiology 75:345–355
Lerou JG, Verheijen R, Booij LH (2002) Model-based administration of inhalation anaesthesia. 4. Applying the system model. Br J Anaesth 88:175–183
Levitt DG, Schnider TW (2005) Human physiologically based pharmacokinetic model for propofol. BMC Anesthesiol 5:4
Lin CY (1994) Uptake of anaesthetic gases and vapours. Anaesth Intensive Care 22:363–373
Lockhart SH, Cohen Y, Yasuda N, et al (1991) Cerebral uptake and elimination of desflurane, isoflurane, and halothane from rabbit brain: an in vivo NMR study. Anesthesiology 74:575–580
Lockwood GG, Chakrabarti MK, Whitwam JG (1993) The uptake of isoflurane during anaesthesia. Anaesthesia 48:748–752
Lowe J, Ernst E (1981) The quantitative practice of anesthesia—use of a closed circuit. Williams & Wilkins, Baltimore
Mapleson WW (1998) The theoretical ideal fresh-gas flow sequence at the start of low-flow anaesthesia. Anaesthesia 53:264–272
Morris LE (1994) Closed carbon dioxide filtration revisited. Anaesth Intensive Care 22:345–358
Neckebroek M, Hendrickx J, Deloof T, De Wolf A (2001) Effects of ventilation on the isoflurane inspired-expired gradient during low flow anesthesia. Eur J Anaesthesiol 18:A317
NONMEM Project Group (1992) NONMEM user's guide. University of California at San Francisco
Park JY, Kim JH, Kim WY, et al (2005) Effect of fresh gas flow on isoflurane concentrations during low-flow anaesthesia. J Int Med Res 33:513–519
Rehberg B, Bouillon T, Zinserling J, Hoeft A (1999) Comparative pharmacodynamic modeling of the electroencephalography-slowing effect of isoflurane, sevoflurane, and desflurane. Anesthesiology 91:397–405
Rietbrock S, Wissing H, Kuhn I, Fuhr U (2000) Pharmacokinetics of inhaled anaesthetics in a clinical setting: description of a novel method based on routine monitoring data. Br J Anaesth 84:437–442
Sani O, Shafer SL (2003) MAC attack? Anesthesiology 99:1249–1250
Severinghaus JW (1954) The rate of uptake of nitrous oxide in man. J Clin Invest 33:1183–1189
Shafer SL (1998) Principles of pharmacokinetics and pharmacodynamics. In: Longnecker DE, Tinker JH, Morgan GE Jr (eds) Principles and practice of anesthesiology, 2nd edn. Mosby, St. Louis, p 1173
Slock E, Hendrickx J, Van Zundert A, et al (2003) Effect of carrier gases on isoflurane vaporizer dial settings during minimal flow anesthesia. Eur J Anaesthesiol 30:A453
Sobreira DP, Jreige MM, Saraiva R (2001) The fresh-gas flow sequence at the start of low-flow anaesthesia. Anaesthesia 56:379–380
Stoelting RK, Longnecker DE, Eger EI (1970) Minimum alveolar concentrations in man on awakening from methoxyflurane, halothane, ether and fluroxene anesthesia: MAC awake. Anesthesiology 33:5–9

Tempia A, Olivei MC, Calza E, et al (2003) The anesthetic conserving device compared with conventional circle system used under different flow conditions for inhaled anesthesia. Anesth Analg 96:1056–1061

Varvel JR, Donoho DL, Shafer SL (1992) Measuring the predictive performance of computer-controlled infusion pumps. J Pharmacokinet Biopharm 20:63–94

Vermeulen P (2000) Tuning a physiological model for closed-circuit anaesthesia. PhD thesis. University of Utrecht, pp 41–67

Vermeulen PM, Lerou JG, Dirksen R, et al (1995) A system model for halothane closed-circuit anesthesia. Structure considerations and performance evaluation. Anesthesiology 83:515–527

Vermeulen PM, Lerou JG, Dirksen R, et al (1997) Repeated enflurane anaesthetics and model predictions: a study of the variability in the predictive performance measures. Br J Anaesth 79:488–496

Virtue RW (1974) Minimal-flow nitrous oxide anesthesia. Anesthesiology 40:196–198

Westenskow DR, Jordan WS, Hayes JK (1983) Uptake of enflurane: a study of the variability between patients. Br J Anaesth 55:595–601

Wissing H, Kuhn I, Rietbrock S, Fuhr U (2000) Pharmacokinetics of inhaled anaesthetics in a clinical setting: comparison of desflurane, isoflurane and sevoflurane. Br J Anaesth 84:443–449

Yasuda N, Targ AG, Eger EI (1989) Solubility of I-653, sevoflurane, isoflurane, and halothane in human tissues. Anesth Analg 69:370–373

Yasuda N, Lockhart SH, Eger EI, et al (1991a) Kinetics of desflurane, isoflurane, and halothane in humans. Anesthesiology 74:489–498

Yasuda N, Lockhart SH, Eger EI, et al (1991b) Comparison of kinetics of sevoflurane and isoflurane in humans. Anesth Analg 72:316–324